

1 **Assessing the adaptative potential to temperature and precipitation along a steep**
2 **environmental gradient in populations of European beech**

3
4 **Mila Tost**^{1,2,3} (0009-0001-3460-5994), **Ourania Grigoriadou-Zormpa**^{2,3} (0009-0000-2994-0643), **Selina**
5 **Wilhelmi**^{2,3} (0000-0001-7640-6523), **Markus Müller**^{2,3} (0000-0001-9990-0719), **Henning Wildhagen**⁴ (0000-
6 0003-4970-8539), **Alexandru Lucian Curtu**⁵ (0000-0001-8509-279X), **Oliver Gailing**^{2,3} (0000-0002-4572-2408)

7
8 ¹⁾ Division of Plant Breeding Methodology, University of Göttingen, Carl-Sprengel-Weg 1, 37075 Göttingen
9 (Germany).

10 ²⁾ Forest Genetics and Forest Tree Breeding, University of Göttingen, Büsgenweg 2, 37077 Göttingen (Germany).

11 ³⁾ Center for Integrated Breeding Research (CiBreed), University of Göttingen,
12 Von-Siebold-Str. 4, 37075 Göttingen (Germany).

13 ⁴⁾ Faculty of Resource Management, HAWK, Büsgenweg 1a, 37077 Göttingen (Germany).

14 ⁵⁾ Department of Silviculture, Transilvania University of Brasov, Sirul Beethoven -1, Braşov 500123 (Romania).

15

16 ***Corresponding author:** Oliver Gailing (ogailin@gwdg.de)

17 **Running title:** Adaptation in European beech

18 **Key words:** local adaptation, environmental association analysis, *Fagus sylvatica*, climate change

19

20

21 **Abstract**

22 Climate change poses a significant threat to European beech. These concerns highlight the need to assess the adaptive
23 potential of European beech populations to climate change. Landscape genomics, also known as environmental
24 association analysis, is a powerful tool for identifying gene loci that contribute to local adaptation to environmental
25 pressures. Genotypic data was collected from ~100 adult beech trees per stand in five locations in the South-Eastern
26 Romanian Carpathians along an altitudinal gradient associated with precipitation and temperature. In total, 53
27 environmental variables, comprising frost frequency change, temperature and precipitation, were extracted from the
28 climatology data base CHELSA. Based on these variables the Ellenberg-Quotient (EQ) was calculated. We performed
29 environmental association analysis using LFMM (latent factor mixed models) to identify Single Nucleotide
30 Polymorphism (SNP) markers associated with environmental variables and with the principal components calculated
31 based on these. We identified 446 SNP markers significantly associated with the first principal component (PC). These
32 were overlapping with the SNP markers significantly associated with all environmental variables except precipitation
33 accumulated during the growing season. The first PC was correlated with all temperature-based variables and elevation
34 at $|r| \sim 0.989$ to ~ 0.997 and with all precipitation-based and Ellenberg-Quotient variables at $|r| \sim 0.945$ to 0.950 , except
35 precipitation accumulated during the growing season. A high peak region on chromosome 2 from ~ 4.56 to ~ 16.27 Mb
36 appeared in all results. This region was ~ 3.47 Mb downstream from a region for local adaptation identified by Lazic
37 et al. (2024). In this peak, 273 markers located in the coding region of 22 genes were found. Ten out these 22 were
38 described based on a literature review. Among these ten genes, two may be involved in local adaptation based on our
39 literature review. These two genes are *polygalacturonase QRT3-like* and *NRT1/PTR_FAMILY 5.4-like*. The gene
40 *polygalacturonase QRT3-like* plays a role in pollen development in *Arabidopsis thaliana* L. and *Brassica rapa* L. We
41 observed at the corresponding SNP markers, a correlation of the minor allele frequency and temperature-based
42 environmental variables.

43 **Introduction**

44 Many forest tree species are negatively affected by the direct impact of drought stress due to climate change (Hartmann
45 et al. 2022; Piedallu et al. 2023). Published observations also report that European beech (*Fagus sylvatica* L.) shows
46 increased mortality due to more frequent summer droughts (Martinez del Castillo et al. 2022). European beech is
47 distributed across large parts of Europe and can be found from the south of Italy up to the south of Norway (Houston
48 Durrant et al. 2016). It is one of the most important forest tree species in Europe, accounting for the highest percentage
49 of broadleaf growing stock on the continent (Houston Durrant et al. 2016; FAO 2020; Rukh et al. 2023). Martinez del
50 Castillo et al. (2022) report that the 1°C increase in temperature from 1955-1985 to 1986-2016 led to reduced beech
51 tree growth at higher altitudes in Central Europe, such as along the Carpathians. Hartmann et al. (2022) describe that
52 European beech forests in central Germany are suffering due to increased late frost events in montane regions.
53 Projections assume a decline in the environmental suitability of beech in south and central Germany (Baumbach et al.
54 2019) and southern Europe (Martinez del Castillo et al. 2022).

55
56 Hence, the importance of studying the adaptive potential of forests to changing climatic conditions by evaluating
57 adaptive loci and their association with environmental variables is increasing (Neale and Kremer 2011). Landscape
58 genomics also deemed as environmental association analysis (EAA) aims to identify loci involved in local adaptation
59 and associated with environmental variables (Frichot et al. 2013; Berg and Coop 2014; Rellstab et al. 2015). Many
60 methods are available for EAA which comprise Bayenv (Berg and Coop 2014) and latent factor mixed models (LFMM)
61 (Frichot et al. 2013; Frichot and François 2015). Both methods report low rates of false positive observations in
62 comparison to other EAA methods, because they include correction methods for population structure (Frichot et al.
63 2013; De Villemereuil et al. 2014). Most EAA methods have difficulties to distinguish effects of local adaptation from
64 genetic drift and demographic history (Hancock et al. 2008). Neutral markers are then used as a null distribution
65 (Hancock et al. 2008). So-called neutral markers comprise intergenic markers which are not in close proximity to genes
66 and are therefore assumed to only capture genetic variation due to genetic drift and demographic history, but not due
67 to adaptation (Hancock et al. 2008). Neutral markers are, however, difficult to identify and intergenic regions do not
68 necessarily only capture genetic variation due to genetic drift and demographic history (Frichot et al. 2013). This is
69 even more difficult with sequencing methods like single primer enrichment technology (SPET) that are designed in
70 particular for SNPs within and close to genes (Scaglione et al. 2019). LFMM addresses this problem of confounding
71 effects of genetic drift and demographic history by testing the correlation between environmental and genetic variation

72 while estimating the effects of hidden factors such as residual levels of population structure (Frichot et al. 2013). EAA
73 methods return SNP markers which are associated with tested environmental variables (Frichot et al. 2013; Rellstab et
74 al. 2015). Identified SNPs could help to detect genes or loci involved in adaptation to specific environmental pressures
75 and be compared to other studies. Previous studies in European beech investigated adaptation to different environments
76 with F_{ST} outlier approaches (Csilléry et al. 2014; Krajmerová et al. 2017; Cuervo-Alarcon et al. 2018). Some more
77 recent studies used LFMM and other EAA methods but did not work with the chromosome-level genome assembly of
78 European beech (Postolache et al. 2021; Müller et al. 2024). The chromosome-level genome assembly of European
79 beech enabled us to perform a comprehensive analysis of the identified genes. Only few studies used LFMM and other
80 EAA methods and worked with SNP marker data sets based on the chromosome-level genome assembly of European
81 beech (Lazic et al. 2024).

82
83 Sampling for EAA studies is often done along environmental gradients (Rellstab et al. 2015). For this study, we used
84 497 individual trees from five European beech stands in the South-Eastern Romanian Carpathians sampled along an
85 altitudinal gradient ranging from 550 up to 1400 m above sea level associated with precipitation and temperature. In
86 total, 53 environmental variables were investigated separately in EAA by using LFMM. Additionally, we also
87 performed a principal component analysis (PCA) on all environmental variables. Performing a PCA on environmental
88 variables can help to reduce the data set and to decrease the number of tests (Rellstab et al. 2015). Though, the
89 interpretation of the principal components (PCs) can be difficult and true positives may be missed, leading to
90 misclassifications (Rellstab et al. 2015). It is recommended to only run EAA on environmental PCs when they can be
91 interpreted (Rellstab et al. 2015).

92
93 The climatic conditions in the summer of the South-Eastern Romanian Carpathians may be similar to the future climatic
94 conditions in mountainous regions of Germany (Baumbach et al. 2019; Martinez del Castillo et al. 2022). Patterns of
95 fine-scale local adaptation to different environmental pressures will be described along a steep environmental gradient
96 in these populations of European beech. Furthermore, environmental variables involved in local adaptation will be
97 identified. Results from this study can help in the adaptive management of European and German beech forests, but
98 there is still a remaining uncertainty regarding the future climatic conditions (Jandl et al. 2019).

99

100 **Material and methods**

101 **Data sampling and stand descriptions**

102 The used data set consists of 497 individual trees collected from five beech stands in the South-Eastern Romanian
103 Carpathians along an altitudinal gradient associated with precipitation and temperature. The beech stands are referred
104 to as Lempes, Tampa, Solomon, Lupului and Ruia. In each stand, approximately 100 trees were sampled in August
105 2021 for DNA analyses. Lempes was the lowest elevation site at 550 to 600 m, followed by Tampa located at 650-700
106 m, Solomon at 800 to 900 m and Lupului at 1000 to 1150 m. Ruia was the highest location at 1300 to 1450 m. The
107 stands are naturally regenerating and were established between 100 to 160 years ago. Ruia and Lupului were
108 established 150 and 160 years ago. Solomon, Tampa and Lempes were established 110 to 130, 130 to 150 and 100
109 years ago (Grigoriadou-Zormpa et al. 2024). The diameter at breast height (DBH) in Ruia is on average 35.69 cm, in
110 Lupului 52.52 cm, in Solomon 29.52 cm, in Tampa 41.28 cm and in Lempes 47.51 cm. The distribution of DBH
111 measurements across the different stands is available in supplemental Figure S1. For further details see Grigoriadou-
112 Zormpa et al. (2024), in which also fine-scale spatial genetic structure of the stands is reported.

113

114 **Genotypic data**

115 Individual trees were sequenced by using the single primer enrichment technology (SPET) (Scaglione et al. 2019).
116 This sequencing method targets SNPs located within and close to genes and flanking regions of ± 2 kb (Scaglione et
117 al. 2019). The target regions were determined by previous whole-genome sequencing of a subset of 96 individual trees
118 by IGATech (IGA Technology Services Srl, Udine, Italy). Reads were aligned to the *Fagus sylvatica* L. reference
119 genome version 2 (Mishra et al. 2022) by using BWA-MEM v0.7.17 (Li and Durbin 2009). Only aligned reads with a
120 mapping quality ≥ 10 were kept and duplicated reads were removed. Variant calling was done along with filtering for
121 minimum read number of an allele in a sample with Freebayes v1.3.6 (Garrison and Marth 2012; Grigoriadou-Zormpa
122 et al. 2024). Normalization and filtering for raw read depth were performed using bcftools (Danecek et al. 2011;
123 Grigoriadou-Zormpa et al. 2024). After this, a total of 838,522 SNP markers were kept, which were used in the
124 downstream analysis.

125

126 **Environmental data**

127 In total, 53 environmental variables were used in this analysis. The environmental variables comprise recorded weather
128 data from 1981 until 2010. Environmental data was downloaded from the climatology data base CHELSA v2.1 (Karger

129 et al. 2017; Karger et al. 2018; Karger et al. 2020a; Karger et al. 2020b; Beck et al. 2020; Brun et al. 2022). The
130 environmental variables comprised elevation in m above sea level, frost change frequency (fcf), and precipitation and
131 temperature variables (Karger et al. 2017; Karger et al. 2018; Karger et al. 2020a; Karger et al. 2020b; Beck et al.
132 2020; Brun et al. 2022). All these variables were available for groups of individual trees, because the coordinates of
133 the trees were recorded and the climatology data base CHELSA v2.1 has a very high resolution (30 arc sec, ~1km).

134
135 Additionally, the Ellenberg-Quotient was calculated as $Q_E = \frac{\text{Temperature in } ^\circ\text{C (July)} * 1000}{\text{Precipitation in mm (mean)}}$ (Ellenberg 2009).

136 Precipitation was modelled as monthly precipitation from January to December, mean annual precipitation and the
137 precipitation accumulated over the growing season (gsp) (Karger et al. 2017; Karger et al. 2018; Karger et al. 2020a;
138 Karger et al. 2020b; Beck et al. 2020; Brun et al. 2022). The temperature was measured as mean, minimum and
139 maximum daily air temperature from January to December (Karger et al. 2017; Karger et al. 2018; Karger et al. 2020a;
140 Karger et al. 2020b; Beck et al. 2020; Brun et al. 2022). The distribution of environmental variables across stands is
141 shown in supplemental Figure S2.

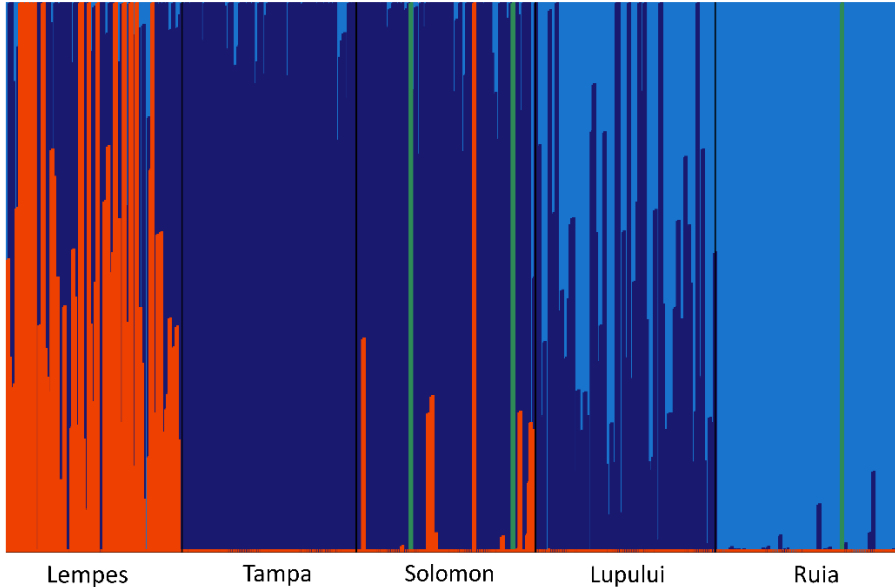
142
143 We examined the correlations of the environmental variables with each other, which are shown in supplemental Figure
144 S3. Correlations were analyzed using R version 4.3.1 (R Core Team 2024). A principle component analysis (PCA)
145 was performed on all 53 environmental variables by using the *prcomp()* R function in the R version 4.3.1 (R Core
146 Team 2024). The first 14 principal components (PCs) with the largest eigenvalues were also investigated using LFMM.
147 Supplemental Figure S4 shows the two first PCs of the PCA on the environmental variables and the eigenvalues of all
148 PCs.

149
150 **Environmental association analysis (EAA)**

151 To test for associations between SNPs and environmental gradients, we used the latent factor mixed models (LFMM)
152 (Frichot et al. 2013) implemented in LEA (Landscape and Ecological Association Studies) R package (R Core Team
153 2024; Frichot and François 2015). This LFMM model is an improved version of the LFMM algorithm from Frichot et
154 al. (2013), which implements LFMM based on a Bayesian bootstrap approach (Frichot and François 2015). LFMM
155 detects correlations between environmental variables and genetic variation while considering random effects due to
156 population structure (Frichot et al. 2013). LFMM estimates confounders also referred to as latent factors (Frichot et al.

157 2013; Frichot and François 2015). Latent factors are then included in a statistical model for testing associations between
158 genotypes and the environmental variable (Frichot et al. 2013; Frichot and François 2015). To run LFMM, missing
159 data had to be imputed (Frichot et al. 2013; Frichot and François 2015), after removal of markers with a missingness
160 >0.05 (see supplemental Fig. S5). Imputation was then done with the *impute()* function from the LEA R package (R
161 Core Team 2024; Frichot and François 2015). LFMM tested all 53 environmental variables and 14 environmental PCs
162 separately (Frichot et al. 2013; Frichot and François 2015). The number of latent factors was set to three based on the
163 results of the population structure analysis (see Fig. 1 and below). LFMM results were then Benjamini-Hochberg (BH)
164 corrected (Benjami and Hochberg 1995). BH correction was conducted with FDRestimation R package (Murray and
165 Blume 2021). To determine whether the significance thresholds are appropriate, the number of false-positive
166 observations exceeding these thresholds was determined by permutation tests. For these permutation tests, the first
167 environmental PC was used. The permutation was performed while maintaining the population or stand structure, with
168 the order of the stands randomized. The stands were randomized by changing the order along the altitudinal gradient
169 to remove association with the altitudinal gradient. This randomization scheme is shown in supplemental Table S6.
170 Additionally, the order of individuals within the stands was randomized by using the *sample()* R function in the R
171 version 4.4.0 (R Core Team 2025). A total of ten replication schemes with ten replications each were carried out. The
172 results of the randomizations are shown in supplemental Table S6. For the significance thresholds based on the BH
173 correction, an average of ~39 false-positive results were observed for the ten different permutations with ten
174 replications (supplementary Table S6).

175
176 **Assessing population stratification and assesment of confounders**
177 To interfeer population structure and to identify the number of confounders in the data set, the fastStructure algorithm
178 was used (Raj et al. 2014). FastStructure uses variational Bayesian inference methods to determine the underlying
179 ancestry proportions, similar to Structure (Pritchard et al. 2000), but faster and with a more flexible priority distribution
180 (Raj et al. 2014). FastStructure achieves similar accuracies comparable to ADMIXTURE (Raj et al. 2014).
181 FastStructure was run in python version 3.11.6 (Van Rossum and Drake 2009). The results were analyzed using R
182 version 4.3.1 (R Core Team 2024). Results of the population structure analysis are shown in Figure 1. There is a clear,
183 albeit slight, differentiation between the stands showing different proportions of three main genetic clusters (Fig. 1).
184



185
186 **Fig. 1:** Population structure based on fastStructure (Raj et al. 2014) of the analyzed five beech stands Lempes, Tampa,
187 Solomon, Lupului and Ruia. The different colors represent the identified clusters based on the population structure
188 analysis.
189

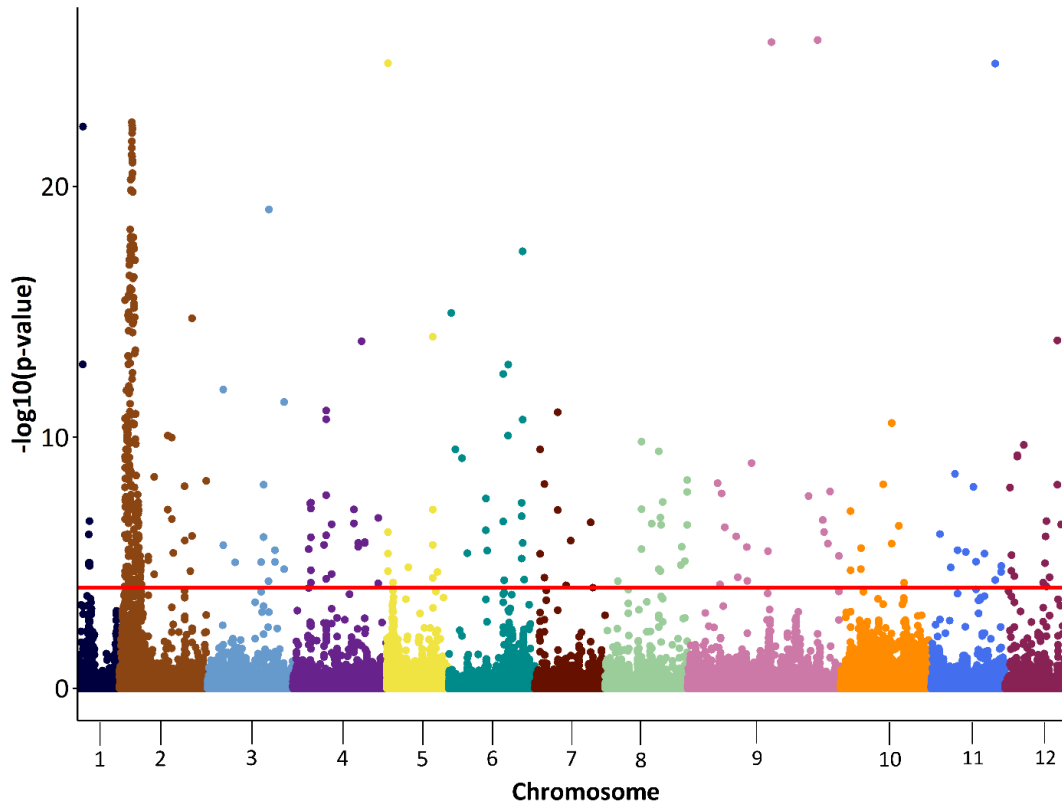
190 Additionally, we conducted an analysis of molecular variance (AMOVA) to assess the variation among stands and
191 within stands with the poppr R package (Kamvar et al. 2013). According to the analysis of molecular variance
192 (AMOVA) the variation among stands was 3.11% and between samples within stands was 96.89% (see supplemental
193 Table S7). The pairwise F_{ST} matrix is shown in supplemental Table S8. The pairwise F_{ST} matrix was calculated based
194 on the StAMPP R package (Pembleton et al. 2013).

195 196 **Results**

197 The first environmental principal component (PC) explained 9.5% of the total variance and the first two PCs accounted
198 together for 15% (see supplemental Fig. S3). Nonetheless, the LFMM results based on these PCs look very similar,
199 and we observed that additional LFMM analysis on subsequent environmental PCs did not yield additional significant
200 associations (see supplemental Fig. S9). The first environmental PC was correlated at $|r| \sim 0.989$ to ~ 0.997 with all
201 temperature-based variables and elevation and at $|r| \sim 0.950$ to ~ 0.945 with all precipitation-based variables and EQ.
202 The correlation coefficients with frost frequency change (fcf) and precipitation accumulated over the growing season
203 (gsp) were $|r| \sim 0.813$ and ~ 0.692 .

204

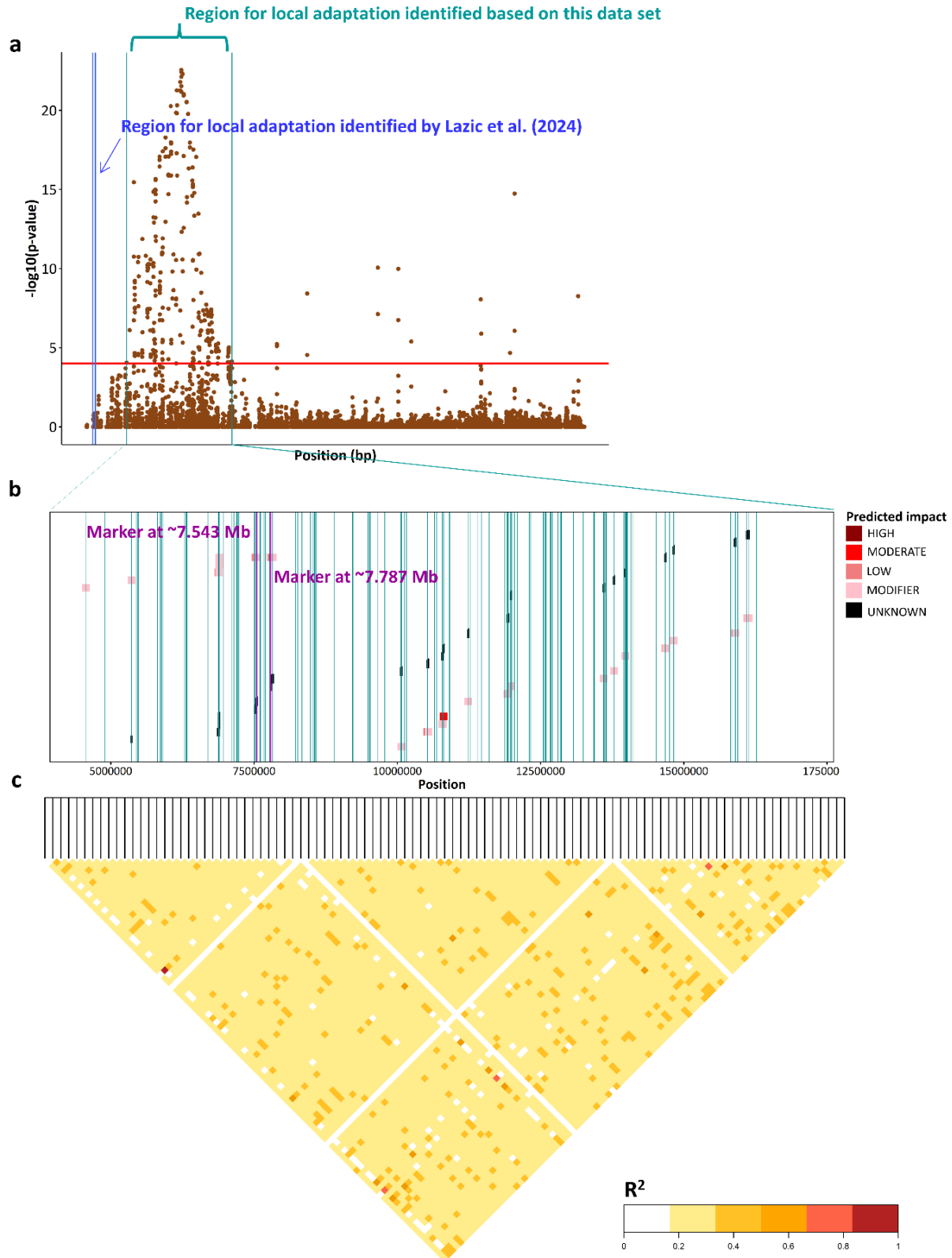
205 Figure 2 shows the results of the LFMM analysis of the first environmental PC with Benjamini-Hochberg (BH)
206 corrected p-values on the $-\log_{10}$ scale. Environmental PC1 was significantly associated with 446 markers, of which
207 288 are located on chromosome 2 (Fig. 2). A high peak region appears on chromosome 2 from ~4.56 to ~16.27 Mb,
208 in which 273 markers are located. The LFMM analysis of the individual environmental variables shows a similar
209 pattern except for gsp (see supplemental Fig. S10).
210



211
212 **Fig. 2:** Manhattan plots based on LFMM results for environmental PC1 with Benjamini-Hochberg (BH) corrected p-
213 values on the $-\log_{10}$ scale. The red horizontal line indicates significance thresholds with $p \leq 0.0001$.
214

215 Figure 3A shows the LFMM results with Benjamini-Hochberg (BH) corrected p-values on the $-\log_{10}$ scale only for
216 chromosome 2. The pairwise linkage disequilibrium (LD) heatmap was calculated for the high peak region on
217 chromosome 2 from ~4.56 to ~16.27 Mb (Fig. 3C). The blue vertical line shows the region for local adaptation observed
218 in a study by Lazic et al. (2024) from 0.79 Mb to 1.09 Mb on chromosome 2. The coding regions of all gene variants
219 observed across this region are shown in Figure 3B. The pairwise LD was 0.2586 in Ruia, 0.2503 in Lupului, 0.2687
220 in Solomon, 0.2620 in Tampa and 0.2668 in Lempes (Fig. 3C).

221
9



222
223 **Fig. 3:** High peak region on chromosome 2 from ~4.56 to ~16.27 Mb with **a**) Benjamini-Hochberg (BH) corrected p-
224 values on the $-\log_{10}$ scale (red horizontal line indicates significance thresholds with $p \leq 0.0001$), the blue vertical line
225 shows the region for local adaptation observed in Lazic et al. (2024), **b**) the coding regions of underlying genes and
226 significant markers (green vertical lines) and **c**) the LD heat map in this region for Solomon.

227 Table 1 shows all significant SNP associations on chromosome 2 within the high peak region. In total, we observed
 228 237 SNP markers located between ~4.56 Mb and ~16.27 Mb. Some markers were located within coding regions of 22
 229 different genes, many markers were located within the coding region of the same gene, and some markers were outside
 230 of the coding regions of genes (Fig. 3). In total, we found ten described genes based on our literature review (Table 1).
 231

232 **Table 1:** List of candidate SNPs with gene annotations associated with environmental PC1 with Bonferroni-Hochberg
 233 corrected p-values at a significance levels of $p \leq 0.0001$ and their annotated gene variants, the underlying genes with
 234 their locations, functions and predicted impact with HIGH, MOD (moderate) and LOW based on SnpEff (Cingolani
 235 et al. 2012). Candidate genes that may be involved in local adaptation are highlighted in bold face.

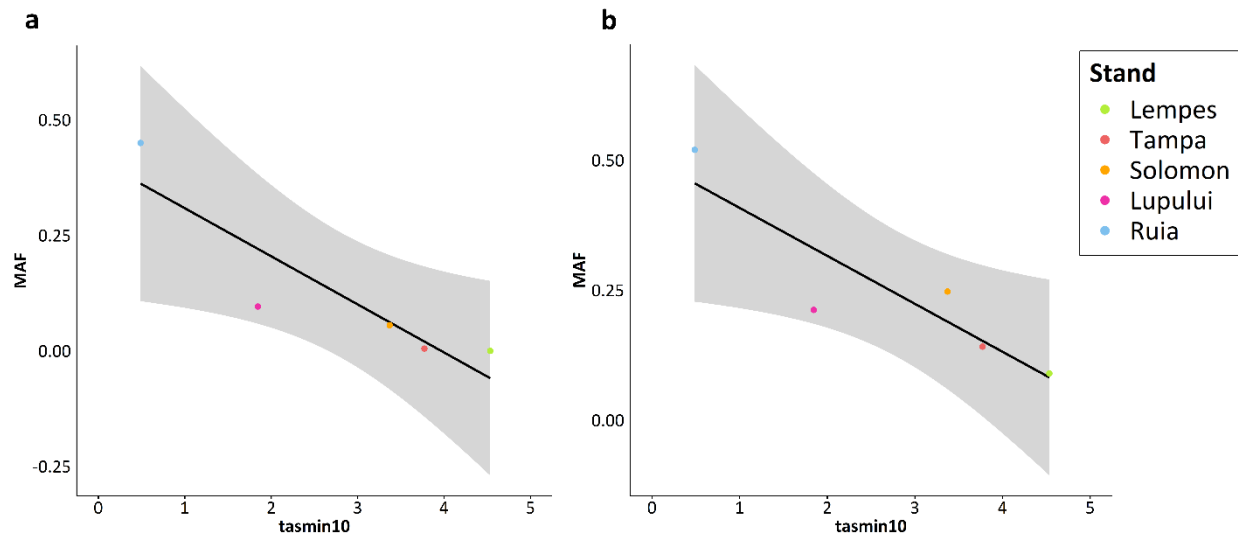
Chr	Marker pos	Gene variant		Underlying gene	Gene description	
2	4560315	Bhaga_2.g515	1 missense variant	MOD	XP_023914361.1	NA
	5362037	Bhaga_2.g604	Stop gain variant	HIGH	PSS09972.1	NA
	5362045		2 missense variants	MOD		
	5362069			MOD		
	6876799	Bhaga_2.g787	1 missense variant	MOD	RWR85963.1	NA
	6886424	Bhaga_2.g788	2 missense variants	MOD	XP_023921788.1	NA
	6886446			MOD		
	6890020	Bhaga_2.g789	1 missense variant	MOD	KAB1227540.1	NA
	7513043	Bhaga_2.g853	1 missense variant	MOD	RVW44103.1	NA
	7542764	Bhaga_2.g857	1 missense variant	MOD	XP_030966603.1	polygalacturonase QRT3-like: responsible for degrading the pollen mother cell wall during microspore development (Rhee et al. 2003, NCBI 2025).
	7787374	Bhaga_2.g883	1 missense variant	MOD	XP_030961693.1	protein NRT1/ PTR FAMILY 5.4-like: functions as a transporter of indole-3-butyric acid (IBA), a precursor of the major endogenous auxin indole-3-acetic acid (IAA) (NCBI 2025)
	7820389	Bhaga_2.g885	1 missense variant	MOD	XP_023871679.1	
	10071121	Bhaga_2.g1122	2 missense variants	MOD	KAE8713369.1	uncharacterized LOC120113939
	10071153			MOD		
	10526069	Bhaga_2.g1166	2 missense variants	MOD	XP_030967199.1	transcription elongation factor SPT6 homolog
	10533078			MOD		

10784123	Bhaga_2.g1189	Variant hits 5'UTR region with premature start codon gain variant	LOW	XP_023872570.1	NA
10805547	Bhaga_2.g1191	2 missense variants	MOD	PON69882.1	NA
10805606			MOD		
11233581	Bhaga_2.g1238	Variant hits 5'UTR region with premature start codon gain variant	LOW	NA	NA
11928940	Bhaga_2.g1303	1 missense variant	MOD	XP_023875148.1	NAD-dependent malic enzyme 62 kDa isoform, mitochondrial
11988800	Bhaga_2.g1308	1 missense variant	MOD	XP_012833939.1	ras-related protein RABH1b
13600231	Bhaga_2.g1485	1 missense variant	MOD	RVX03908.1	NA
13781237	Bhaga_2.g1505	1 missense variant	MOD	XP_023915086.1	NA
13976512	Bhaga_2.g1525	1 missense variant	MOD	XP_023880346.1	NA
14682297	Bhaga_2.g1609	1 missense variant	MOD	XP_030966443.1	spindle and kinetochore- associated protein 1 homolog
14823027	Bhaga_2.g1623	1 missense variant	MOD	XP_030961900.1	protein IWS1 homolog
15894816	Bhaga_2.g1733	1 missense variant	MOD	XP_030963279.1	protein transport protein SEC16B homolog
16129816	Bhaga_2.g1756	1 missense variant	MOD	XP_030965516.1	CCR4-NOT transcription complex subunit 1

236

237 For the markers on chromosome 2 at ~ 7.543 Mb and at ~ 7.787 Mb, we found two interesting underlying candidate
238 genes that may be involved in local adaptation. At both markers, the minor allele frequency (MAF) decreases with
239 increasing minimum daily temperature in October following the altitudinal gradient (Fig. 4). For minimum daily
240 temperature in October, we observed the highest absolute correlation coefficients of $|r| \sim 0.9055$ (p-value = 0.03) and
241 ~ 0.9261 (p-value = 0.024). Significant correlation coefficients of the MAF and the other environmental variables are
242 shown in supplemental Figure S11. For all temperature-based variables, frost change frequency (fcf) and Ellenberg-
243 Quotient (EQ), we observed the same trend (see supplemental Fig. S11 and Table S12). For all precipitation-based
244 variables and elevation, we observed the opposite trend (see supplemental Fig. S11 and Table S12). The correlation
245 coefficients of the MAF and precipitation-based variables, EQ and fcf were not significant. The significant correlation
246 coefficients ranged between $|r| \sim 0.8786$ and ~ 0.9055 for the marker on chromosome 2 at ~ 7.543 Mb. For the marker
247 on chromosome 2 at ~ 7.787 Mb, the significant correlation coefficients ranged between $|r| \sim 0.9090$ and 0.9261.

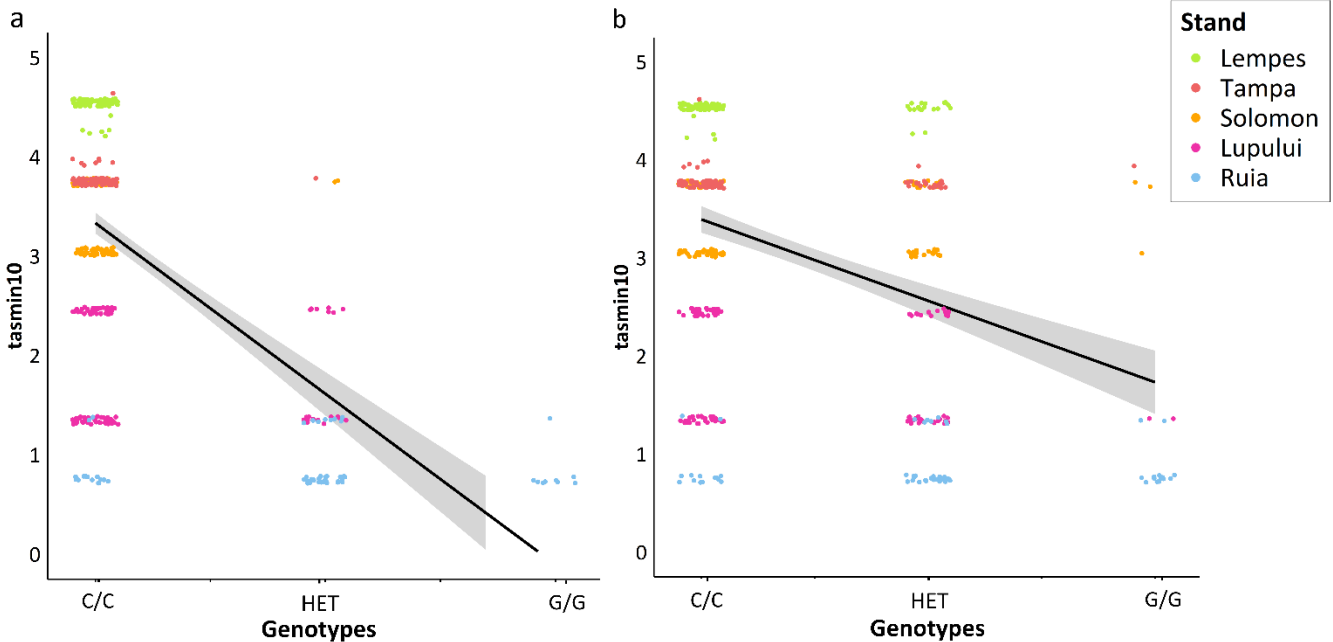
248



249
250 **Fig. 4: a)** Correlation between minimum daily temperature in October (tasmin10) and the minor allele frequency
251 (MAF) of the significant markers ($p \leq 0.0001$) on chromosome 2 at ~ 7.543 Mb with a correlation coefficient of -0.9055
252 (p -value = 0.03). This marker was annotated with gene variant *Bhaga_2.g857*, with the underlying gene
253 *polygalacturonase QRT3-like*. **b)** Correlation between minimum daily temperature in October and the minor allele
254 frequency (MAF) of the significant markers ($p \leq 0.0001$) on chromosome 2 at ~ 7.787 Mb with a correlation coefficient
255 of -0.9261 (p -value = 0.024). This marker was annotated with gene variant *Bhaga_2.g883*, with the underlying gene
256 protein *NRT1/ PTR FAMILY 5.4-like*.

257
258
259 For all other markers on chromosome 2 from ~ 4.56 to ~ 16.27 Mb, we observed the same trend (see supplemental Fig.
260 S13). In all cases, the minor allele frequency (MAF) is correlated with minimum daily temperature in October (see
261 supplemental Fig. S13). Additionally, a linear regression of the different genotypes observed at the SNP markers on
262 chromosome 2 at ~ 7.543 Mb (*Bhaga_2.g857*, with the underlying gene *polygalacturonase QRT3-like*) and ~ 7.787 Mb
263 (*Bhaga_2.g883*, with the underlying gene protein *NRT1/ PTR FAMILY 5.4-like*) and minimum daily temperature in
264 October is shown in Figure 5. The regression coefficients for SNP markers on chromosome 2 at ~ 7.543 Mb and at
265 ~ 7.787 Mb are 0.3468 and 0.1646, respectively (Fig. 5).

266



267
268 **Fig. 5:** Correlation between minimum daily temperature in October (tasmin10) and observed genotypes at the
269 significant SNP markers on chromosome 2 at ~7.543 Mb (*Bhaga_2.g857*, with the underlying gene *polygalacturonase*
270 *QRT3-like*) (a) and 7.787 Mb (*Bhaga_2.g887*, with the underlying gene protein *NRT1/PTR FAMILY 5.4-like*) (b). The
271 coefficients of determination R^2 were 0.3468 ($p \sim 0$) and 0.1646 ($p \sim 0$).
272
273

274 **Discussion**
275 **EAA results strongly correlate with temperature-based variables**
276 This environmental association analysis aims to assess the adaptive potential to different environmental pressures along
277 a steep environmental gradient in populations of European beech from five locations in the South-Eastern Romanian
278 Carpathians. The altitudinal gradient is associated changes in precipitation and temperature (see supplemental Fig. S2).
279 In total, 53 environmental variables and the principal components calculated based on these were used to perform
280 environmental association analysis using LFMM (latent factor mixed models). We identified 446 SNP markers
281 significantly associated with the first principal component (PC). These were overlapping with the SNP markers
282 significantly associated with all environmental variables except precipitation accumulated during the growing season.
283 The first PC was correlated with all temperature-based variables and elevation at $|r| \sim 0.989$ to ~ 0.997 and with all
284 precipitation-based and Ellenberg-Quotient variables at $|r| \sim 0.945$ to 0.950 , except precipitation accumulated during
285 the growing season. The 273 markers on chromosome 2 from ~4.56 to ~16.27 Mb, are overlapping or close to 22
286 genes. In total, we found ten genes with gene descriptions available based on our literature review (Table 1). Most of
287 these genes are involved in gene regulation processes and enzyme catalyzation, and their impact is difficult to deduce

288 (see supplemental Table S14). For some genes, functional studies are only available for homologs in rather distantly
289 related species, such as humans (supplemental Table S14).

290
291 For two gene variants we found annotated genes potentially involved in local adaptation to specific environmental
292 conditions and both genes were studied in plants. These gene variants were *Bhaga_2.g857* and *Bhaga_2.g883*. A high
293 peak region on chromosome 2 from ~4.56 to ~16.27 Mb appeared in all results. This region was ~3.47 Mb downstream
294 from a high-confidence region for local adaptation identified by Lazic et al. (2024) on the same chromosome ~0.79
295 Mb to 1.09 Mb.

296
297 **EEA peak region on chromosome 2 locates close to previously reported high-confidence region for local**
298 **adaptation**

299 Lazic et al. (2024) found the gene variant *Bhaga_2.g.94* which was annotated with the gene *Callose synthase 1*. It was
300 assumed that *Callose synthase 1* may be involved in winter dormancy and spring bud burst (Lazic et al. 2024). *Callose*
301 *synthase 1* is described as being involved in callose deposition, during microspore development. Microspores are
302 surrounded by a callose wall, this wall is then degraded and microspores are released (Tylewicz et al. 2018; Chu et al.
303 2024). We did not observe any significant SNP markers overlapping or in linkage disequilibrium (LD) with the high-
304 confidence region from Lazic et al. (2024). However, we found a candidate gene based on our literature review, with
305 very similar function to *Callose synthase 1* which was annotated for a marker on chromosome 2 at ~7.543 Mb. This
306 candidate gene is *polygalacturonase QRT3-like (Bhaga_2.g857)*. The gene *polygalacturonase QRT3-like* plays a
307 crucial role in pollen development in *Arabidopsis thaliana* L. (Rhee et al. 2003) and *Brassica rapa* L. (Chu et al. 2024).
308 The gene function of *polygalacturonase QRT3-like* is similar to *Callose synthase 1* (Rhee et al. 2003; Tylewicz et al.
309 2018; Chu et al. 2024) and they are often studied together (Rhee et al. 2003; Chu et al. 2024). For further studies we
310 recommend to not only consider the markers from this study, but also the region identified by Lazic et al. (2024). Our
311 results provide statistical support for local adaptation on a small geographic scale in the face of gene flow along an
312 environmental gradient. Lazic et al. (2024) studied local adaptation in 98 populations distributed from Southern Europe
313 until Central and Eastern Europe.

314
315 **The candidate gene *polygalacturonase QRT3-like***

316 The gene variant *Bhaga_2.g857* corresponds to the underlying gene *polygalacturonase QRT3-like* (NCBI 2025). We
317 found one SNP on chromosome 2 at ~7.543 Mb located within the coding region of *Bhaga_2.g857* (*polygalacturonase*
318 *QRT3-like*) (supplemental Fig. S15). At this position of the coding region, a missense variant with moderate impact is
319 located causing a codon change which leads to a change in the polar bonds of the amino acids (supplemental Table
320 S16). The minor allele frequency at this marker decreased with increasing minimum daily temperature in October. The
321 same significant correlation trend was observed for many temperature-based variables (see supplemental Fig. S11).
322 The correlation with precipitation-based variables or other environmental variables like EQ, frost frequency change
323 (fcf) and elevation was not significant. Our results suggest that this gene is involved in local adaptation to temperature.

324
325 Furthermore, a splice region variant of the coding region with low impact of this gene is located 70 bp upstream from
326 the highly significant SNP marker (supplemental Fig. S15). The marker at the position of the splice region variant and
327 the other missense variants are contained as markers in the data set, but are not significant. High LD is observed across
328 the coding region of *Bhaga_2.g857* (*polygalacturonase QRT3-like*), but the LD is incomplete across the entire coding
329 region of the gene (supplemental Fig. S15). It is possible that these markers are not exceeding the significance threshold
330 because of insufficient power of the study (Sun et al. 2022). If very strict significance thresholds are chosen, only the
331 coding region variants with the highest impact and at higher allele frequency in the population will be detected (Sun
332 et al. 2022). In addition to the missense variants already mentioned, there are seven further missense variants between
333 21 bp upstream and 142 bp downstream of the marker (see supplemental Fig. S15).

334
335 The high-confidence region on chromosome 2 from ~0.79 to 1.09 Mb from Lazic et al. (2024) was identified by three
336 different methods for environmental association analysis (EAA). These three methods comprised LFMM from the
337 LEA package (Frichot et al. 2013; Frichot and François 2015), Baypass (Gautier 2015) and WZA (Capblancq and
338 Forester 2021). Additionally, Lazic et al. (2024) also measured the relative expression of *Callose synthase 1* in winter
339 buds of eight beech trees. They observed that the relative expression level of *Callose synthase 1* was increased, but not
340 differentially expressed, in the individuals carrying the alternative allele at the SNP marker identified as top LFMM
341 hit on chromosome 2 at ~0.898 Mb (Lazic et al. 2024). The individual trees carrying the homozygous genotype of the
342 alternative allele at this SNP marker showed in a common garden experiment less days until bud burst (Lazic et al.
343 2024). Furthermore, a clear pattern of geographic distribution across the sampling area from Southern Europe to
344 Central and Eastern Europe was observed (Lazic et al. 2024). The alternative allele was increased towards Central and

345 Eastern Europe, in this region, the temperature of the coldest month was much lower (Lazic et al. 2024). To compare
346 patterns of local adaptation at small and range-wide geographic scales, in future studies we will assess our candidate
347 SNPs also at a larger geographic scale across the species distribution range.

348

349 **The candidate gene *NRT1/PTR_FAMILY 5.4-like***

350 For the gene variant *Bhaga_2.g883*, the annotated gene *NRT1/PTR_FAMILY 5.4-like* was found (NCBI 2025). The
351 gene *NRT1/PTR_FAMILY 5.4-like* belongs to the NRT1/PTR family. This family was initially described as nitrate
352 transporters, but recently their involvement in the transportation of phytohormones like auxin was discovered (Chiba
353 et al. 2015; Watanabe et al. 2020). Many different members of this gene family are studied (Bai et al. 2013; Chiba et
354 al. 2015; Watanabe et al. 2020), but *NRT1/PTR_FAMILY 5.4-like* was not studied in detail to our knowledge. But we
355 can assume that this particular gene may also be involved in the transportation of phytohormones like auxin. The gene
356 *NRT1/PTR_FAMILY* serves as a transporter for indole-3-butyric acid (IBA), which is a precursor of indole-acetic acid
357 (IAA) (Watanabe et al. 2020). IAA is the major form of naturally available auxin (Watanabe et al. 2020; Chiba et al.
358 2015). At the position of the marker on chromosome 2 at ~7.787 Mb, a missense variant with moderate impact was
359 found in the coding region of *Bhaga_2.g883 (NRT1/PTR_FAMILY 5.4-like)* (supplemental Fig. S17). This missense
360 variant causes a codon change which replaces a hydrophilic with a hydrophobic amino acid (supplemental Table S16).
361 This change can increase the stability of the proteins (van Dijk et al. 2015) involved in auxin transport in the Ruia
362 stands. Additionally, one splice region variant of the coding region of *Bhaga_2.g883 (NRT1/PTR_FAMILY 5.4-like)*
363 was located 83 bp upstream from this significant marker (supplemental Fig. S17). This splice region variant was not
364 recognized as significant in our analysis, which could also be due to the fact that it has less influence on the coding
365 region. LD varies strongly across the gene coding region of *Bhaga_2.g883 (NRT1/PTR_FAMILY 5.4-like)*
366 (supplemental Fig. S17). It seems like the splice region variant is not in strong LD with the marker and the rest of the
367 coding region of this gene (supplemental Fig. S17). The missense variant in the coding region is in almost complete
368 LD (~1) with the marker (supplemental Fig. S17).

369

370 Figure 4B shows that the MAF at the marker on chromosome 2 at ~ 7.787 Mb decreased with increasing minimum
371 daily temperature in October. The same trend was observed for all temperature-based variables and also for elevation
372 with a significance level of $p \leq 0.05$. The correlation coefficient for MAF at this marker and precipitation in October
373 was ~0.81 (p -value = 0.096), the correlation coefficients for the other precipitation-based variables except gsp were

374 similar. Auxin activity is decreased during drought stress (Popko et al. 2009). A decrease in free auxin in the cambial
375 zone of poplar was observed in acclimation to drought stress caused by osmotic stress due to changes in water potential
376 in the environment (Popko et al. 2009). In general, high auxin activity is correlated with high growth rates in trees
377 (Popko et al. 2009). Since this particular gene was not studied, it is difficult to draw direct conclusions about the exact
378 involvement in local adaptation, but we would assume that auxin is decreased in the shoot apical meristems of the
379 stands with high drought stress. The allele frequency at the SNP candidate marker on chromosome 2 at ~7.787 Mb is
380 decreased in the stands Lempes, Tampa and Solomon with higher drought stress (see Fig. 4b). Only in Ruia, the allele
381 frequency at the SNP candidate is increased (see Fig. 4b).

382
383 Both gene variants seem to be involved in local adaptation. The LD between the two SNP markers on chromosome 2
384 at ~ 7.543 and ~ 7.787 is 0.6711. The LD across the entire region from ~4.56 to ~16.27 Mb on chromosome 2 varies
385 (Fig. 3). It seems like temperature-based variables are shaping local adaptation much stronger than precipitation-based
386 variables, especially precipitation accumulated over the growing season does not seem to cause strong patterns of local
387 adaptation, at least in these stands.

388
389 The coefficients of determination of the linear regression between SNP genotypes and minimum daily temperature in
390 October on chromosome 2 at ~ 7.543 Mb and at ~7.787 Mb are 0.3468 and 0.1646, respectively (Fig. 5). For the SNP
391 maker at ~ 7.543 Mb, the homozygous G/G genotype only occurs in the high-elevation population Ruia, while the
392 heterozygous genotype C/G is mostly restricted to the high elevation populations Ruia and Lupului. On the other hand,
393 the C/C genotype is present in similar frequencies in all populations. This pattern suggests strong environmental
394 selection. This trend is not as pronounced for the marker at ~7.787 Mb on chromosome 2 (Fig. 5).

395
396 In a genome-wide association study (GWAS) conducted on the same genotyping data set as in this study, we observed
397 significant associations between 101 SNPs located on chromosome 10 and stomatal density as shown in Tost et al.
398 (2025). These 101 markers are located on chromosome 10 in a region spreading from ~4.9 to 13.67 Mb and also appear
399 as one region (Tost et al. 2025). Five genes were located in this region that may play a role in controlling stomatal
400 density (Tost et al. 2025). All markers within this region exhibit similar allele frequencies, which are correlated with
401 stomatal density and the altitudinal gradient of the stands (see Tost et al. 2025). For the trait carbon isotope composition
402 $\delta^{13}\text{C}$ measured in 2020 and 2022, we observed also a peak on chromosome 10, which was much smaller and only

403 resulted in 2020 in two significant SNP marker associations (Tost et al. 2025). Other significant markers associated
404 with leaf nitrogen content or C/N ratio were also located on chromosome 2 but at ~30.26 Mb and ~31.804 Mb, ~14
405 Mb downstream of the region in this study (Tost et al. 2025). For the significant SNP marker on chromosome 2 at
406 ~31.804 Mb associated with C/N ratio measured in 2021, the gene variant *Bhaga_2.g3457* was found based on a
407 literature review. *Bhaga_2.g3457* was annotated as *abscisic-aldehyde oxidase-like* (NCBI 2024). The gene *abscisic-*
408 *aldehyde oxidase-like* is responsible for oxidation of abscisic aldehyde, which is the last step of abscisic acid (ABA)
409 biosynthesis (Seo et al. 2000). Popko et al. (2009) observed under drought stress auxin and abscisic acid (ABA) interact
410 to regulate plant water status in poplar. The markers identified in our EAA and the GWAS do not overlap, possibly
411 due to insufficient power of the analyses and multiple traits under environmental selection.

412

413 **Permutation testing**

414 For the significance thresholds based on the BH correction, an average of 39 false-positive results were observed for
415 the ten different permutations with ten replications (supplementary Table S6). We identified 446 SNP markers
416 significantly associated with the first principal component (PC), which are considered to be putatively true positive
417 observations. Based on our permutation tests, we calculated a false positive rate of ~0.09. This false-positive rate of
418 ~0.09 is relatively low, so we did not adjust the significance thresholds.

419

420 **Conclusions**

421 In conclusion, our research confirms that environmental association analysis (EAA) can identify environmental
422 variables, which contribute to local adaptation. We observed that mainly temperature-based variables were detected
423 with EAA and showed the strongest correlation with minor allele frequency (MAF) at significant SNP markers from
424 the EAA. Consequently, the adaptive potential to temperature along a steep environmental gradient in the European
425 beech populations was relatively high. A region for local adaptation on chromosome 2 from ~4.56 to ~16.27 Mb was
426 identified based on this study and associated with all environmental variables except precipitation accumulated over
427 the growing season. It seems like temperature-based variables shaped local adaptation. The candidate SNP markers on
428 chromosome 2 at ~7.543 (*Bhaga_2.g857*) and at ~7.787 (*Bhaga_2.g883*) were annotated with the genes
429 *polygalacturonase QRT3-like* and *NRT1/PTR_FAMILY 5.4-like*. The gene *polygalacturonase QRT3-like* plays a role
430 in pollen development in Arabidopsis. The gene *NRT1/PTR_FAMILY 5.4-like* belongs to the NRT1/PTR family, which

431 is involved in the transportation of phytohormones like auxin. The MAF observed at these candidate SNP markers is
432 increased especially in Ruia, the population at highest altitude. Both candidate SNP markers are annotated at a part of
433 the coding region of both genes where a codon change replaces a hydrophilic with a hydrophobic amino acid. This
434 codon change may increase the stability of proteins encoded by genes involved in auxin transport and may be involved
435 in pollen development in the Ruia stands. This is very speculative, because in order to substantiate these assumptions,
436 expression levels of the genes need to be measured.

437

438 **Availability of data and materials**

439 Raw data is publicly available at figshare:
440 https://figshare.com/articles/dataset/VCF_file_with_SPET_sequencing_data_of_DroughtMarkers_project/28748924
441 and was published by Tost et al. (2025). Our analysis code is available publicly on github:
442 <https://github.com/milaleonie/DroughtMarkers>.

443

444 **Acknowledgements**

445 We would like to thank all people involved in this project. We are thanking for help in the lab our lab technician
446 Alexandra Dolynska and bachelor and master students Nikolas Heeger, Luca Schwendemann, Merle Kleikamp, Timo
447 Unbehau, and Jonas Daniel. Furthermore, we are thanking Dr. Mehdi Ben Targem, Mihnea-Ioan-Cezar Ciocîrlan,
448 Jürgen Scheuring and Jonah Fels for help with sampling in Romania.

449

450 **Funding**

451 The used data comes from the drought markers project (Reference numbers: 2218WK43B4, 2218WK43A4). This
452 work was financially supported by the Federal Ministry of Food and Agriculture – FNR-Waldklimafonds. The drought
453 markers project is a collaboration between the University of Goettingen (Germany), the HAWK (Germany), the NW-
454 FVA (Germany) and Transilvania University of Brasov (Romania). We utilized the computational resources of the
455 University of Goettingen's GWDG. Open Access funding enabled and organized by Projekt DEAL.

456

457 **Conflict of interest**

458 The authors declare that there is no conflict of interest.

References

- Bai H, Euring D, Volmer K, Janz D, Polle A (2013) The nitrate transporter (NRT) gene family in poplar. *PLoS One* 8 (8): e72126. <https://doi.org/10.1371/journal.pone.0072126>
- Baumbach L, Niamir A, Hickler T, Yousefpour R (2019) Regional adaptation of European beech (*Fagus sylvatica*) to drought in Central European conditions considering environmental suitability and economic implications. *Reg Environ Change* 19 (4):1159–1174. <https://doi.org/10.1007/s10113-019-01472-0>
- Beck HE, Wood EF, McVicar TR, Zambrano-Bigiarini M, Alvarez-Garretón C, Baez-Villanueva O, Sheffield J, Karger DN (2020) Bias correction of global high-resolution precipitation climatologies using streamflow observations from 9372 catchments. *Journal of Climate* 33 (4): 1299–1315. <https://doi.org/10.1175/JCLI-D-19-0332.1>
- Benjamini Y, Hochberg Y (1995) Controlling the false discovery rate: a practical and powerful approach to multiple testing. *Journal of the Royal Statistical Society. Series B* 57 (1):289–300. <https://doi.org/10.1111/j.2517-6161.1995.tb02031.x>
- Berg JJ, Coop G (2014) A population genetic signal of polygenic adaptation. *PLoS Genet* 10(8): e1004412. <https://doi.org/10.1371/journal.pgen.1004412>
- Brun P, Zimmermann NE, Hari C, Pellissier L, Karger DN (2022) Global climate-related predictors at kilometer resolution for the past and future. *Earth System Science Data* 14:5573–5603. <https://doi.org/10.5194/essd-14-5573-2022>
- Capblancq T, Forester BR (2021) Redundancy analysis: A swiss army knife for landscape genomics. *Methods in Ecology and Evolution* 12 (12):2298–2309. <https://doi.org/10.1111/2041-210X.13722>
- Chiba Y, Shimizu T, Miyakawa S, Kanno Y, Koshihara T, Kamiya Y, Seo M (2015) Identification of *Arabidopsis thaliana* NRT1/PTR FAMILY (NPF) proteins capable of transporting plant hormones. *Journal of Plant Research* 128 (4):679–686. <https://doi.org/10.1007/s10265-015-0710-2>
- Chu W, Dong S, Zou J, Huang S, Feng H (2024) Cloning and functional verification of the male sterile gene BrQRT3 in Chinese cabbage. *Plant Science* 346:112154. <https://doi.org/10.1016/j.plantsci.2024.112154>
- Cingolani P, Platts A, Le Wang L, Coon M, Nguyen T, Wang L et al. (2012) A program for annotating and predicting the effects of single nucleotide polymorphisms, SnpEff: SNPs in the genome of *Drosophila melanogaster* strain w1118; iso-2; iso-3. *Fly* 6 (2):80–92. <https://doi.org/10.4161/fly.19695>
- Csilléry K, Lalagüe H, Vendramin GG, González-Martínez SC, Fady B, Oddou-Muratorio S (2014) Detecting short spatial scale local adaptation and epistatic selection in climate-related candidate genes in European beech (*Fagus sylvatica*) populations. *Mol Ecol* 23(19):4696–4708. <https://doi.org/10.1111/mec.12902>
- Cuervo-Alarcon L, Arend M, Müller M, Sperisen C, Finkeldey R, Krutovsky KV (2018) Genetic variation and signatures of natural selection in populations of European beech (*Fagus sylvatica* L.) along precipitation gradients. *Tree Genetics & Genomes* 14 (6). <https://doi.org/10.1007/s11295-018-1297-2>
- Danecek P, Auton A, Abecasis G et al. (2011) The variant call format and VCFtools. *Bioinformatics* 27:2156–2158. <https://doi.org/10.1093/bioinformatics/btr330>
- de Villemereuil P, Frichot É, Bazin É, François O, Gaggiotti OE (2014) Genome scan methods against more complex models: when and how much should we trust them? *Mol Ecol* 23 (8):2006–2019. <https://doi.org/10.1111/mec.12705>
- Ellenberg H (2009) *Vegetation Ecology of Central Europe*. 4th Ed. Cambridge, Cambridge University Press.
- FAO. FOREST EUROPE (2020) *State of Europe's Forests*.

Frichot E, François O (2015) LEA: an R package for landscape and ecological association studies. *Methods in Ecology and Evolution* 6 (8):925–929. <https://doi.org/10.1111/2041-210X.12382>

Frichot É, Schoville SD, Bouchard G, François O (2013) Testing for associations between loci and environmental gradients using latent factor mixed models. *Molecular Biology and Evolution* 30 (7):1687–1699. <https://doi.org/10.1093/molbev/mst063>

Frichot É, Schoville SD, Bouchard G, François O (2013) Testing for associations between loci and environmental gradients using latent factor mixed models. *Molecular Biology and Evolution* 30 (7):1687–1699. <https://doi.org/10.1093/molbev/mst063>

Garrison E, Marth G (2012) Haplotype-based variant detection from short-read sequencing. arXiv preprint; arXiv:1207.3907 [q-bio.GN]. <https://doi.org/10.48550/arXiv.1207.3907>

Grigoriadou-Zormpa O, Wilhelmi S, Vucetic B, Ciocîrlan MIC, Mueller M, Ciocîrlan E, Curtu LA, Targem MB, H Wildhagen H, Gailing O, Budde KB (2024) Differences in fine-scale spatial genetic structure of European beech populations along elevational gradients. PREPRINT (Version 1) available at Research Square [<https://doi.org/10.21203/rs.3.rs-4559673/v1>].

Gautier, M (2015) Genome-wide scan for adaptive divergence and association with population-specific covariates. *Genetics* 201 (4):1555–1579. <https://doi.org/10.1534/genetics.115.181453>

Hancock AM, Witonsky DB, Gordon AS, Eshel G, Pritchard JK, Coop G, Di Rienzo A (2008) Adaptations to climate in candidate genes for common metabolic disorders. *PLoS Genet* 4 (2):e32. <https://doi.org/10.1371/journal.pgen.0040032>

Hartmann H, Bastos A, Das AJ, Esquivel-Muelbert A, Hammond WM, Martínez-Vilalta J et al. (2022) Climate change risks to global forest health: emergence of unexpected events of elevated tree mortality worldwide. *Annu Rev Plant Biol* 73:673–702. <https://doi.org/10.1146/annurev-arplant-102820-012804>

Houston Durrant T, de Rigo D, Caudullo G (2016). *Fagus sylvatica* and other beeches in Europe: distribution, habitat, usage and threats. In: San-Miguel-Ayanz, J, de Rigo D, Caudullo G, Houston Durrant T, Mauri A. (Eds.), *European Atlas of Forest Tree Species* (Luxembourg). pp 94-95.

Jandl R, Spathelf P, Bolte A, Prescott CE (2019) Forest adaptation to climate change—is non-management an option? In *Annals of Forest Science* 76 (2). <https://doi.org/10.1007/s13595-019-0827-x>

IGA Technology Services Srl, Udine, Italy. <https://igatechnology.com/>.

Kamvar ZN, Brooks JC, Grünwald NJ (2015) Novel R tools for analysis of genome-wide population genetic data with emphasis on clonality. *Front Genet* 6:208. <https://doi.org/10.3389/fgene.2015.00208>

Karger DN, Conrad O, Böhner J et al. (2017) Climatologies at high resolution for the earth's land surface areas. *Scientific Data* 4:170122. <https://doi.org/10.1038/sdata.2017.122>

Karger DN, Zimmermann NE (2018) CHELSAcruts – High resolution temperature and precipitation timeseries for the 20th century and beyond. *EnviDat*. <https://doi.org/10.16904/envidat.228.v2.1>

Karger DN, Dabaghchian B, Lange S, Thuiller W, Zimmermann NE, Graham CH (2020a) High resolution climate data for Europe. *EnviDat*. <http://dx.doi.org/doi:10.16904/envidat.150>

Karger DN, Schmatz D, Dettling G, Zimmermann NE (2020b) High resolution monthly precipitation and temperature timeseries for the period 2006-2100. *Scientific Data*. <https://doi.org/10.1038/s41597-020-00587-y>

Krajmerová D, Hrivnák M, Ditmarová L, Jamnická G, Kmet' J, Kurjak D, Gömöry D (2017) Nucleotide polymorphisms associated with climate, phenology and physiological traits in European beech (*Fagus sylvatica* L.). *New Forests* 48(3):463–477. <https://doi.org/10.1007/s11056-017-9573-9>

Kruszka P, Berger SI, Weiss K, Everson JL, Martinez AF, Hong S et al. (2019) A CCR4-NOT transcription complex subunit 1, CNOT1, variant associated with holoprosencephaly. *Am J Hum Genet* 104 (5):990–993. <https://doi.org/10.1016/j.ajhg.2019.03.017>

Lazic D, Geßner C, Liepe KJ, Lesur-Kupin I, Mader M, Blanc-Jolivet C et al. (2024) Genomic variation of European beech reveals signals of local adaptation despite high levels of phenotypic plasticity. *Nature Commun* 15 (1), p. 8553. <https://doi.org/10.1038/s41467-024-52933-y>.

Liu ZG, Zhou ZW, Chen GH, Bao SL (2007) A putative transcriptional elongation factor hIws1 is essential for mammalian cell proliferation. *Biochem Biophys Res Commun* 353 (1):47–53. <https://doi.org/10.1016/j.bbrc.2006.11.133>

Li H, Durbin R (2009) Fast and accurate short read alignment with Burrows-Wheeler transform. *Bioinformatics* 25: 1754–1760. <https://doi.org/10.1093/bioinformatics/btp324>

Martinez del Castillo E, Zang CS, Buras A, Hacket-Pain A, Esper J, Serrano-Notivoli R et al. (2022) Climate-change-driven growth decline of European beech forests. *Commun Biol* 5 (163). <https://doi.org/10.1038/s42003-022-03107-3>

Mishra B, Ulaszewski B, Meger J, Aury JM, Bodénès C, Lesur-Kupin I et al. (2021) A chromosome-level genome assembly of the European beech (*Fagus sylvatica*) reveals anomalies for organelle DNA integration, repeat content and distribution of SNPs. *Front Genet* 12. <https://doi.org/10.3389/fgene.2021.691058>.

Murray MH, Blume JD (2021) FDRestimation: Flexible false discovery rate computation in R. *F1000Research* 10, p. 441. <https://doi.org/10.12688/f1000research.52999.2>

National Center for Biotechnology Information (NCBI). Bethesda (MD): National Library of Medicine (US), National Center for Biotechnology Information. <https://www.ncbi.nlm.nih.gov/>. Accessed 22 January 2025.

Neale DB, Kremer A (2011) Forest tree genomics: growing resources and applications. In *Nature reviews. Genetics* 12 (2):111–122. <https://doi.org/10.1038/nrg2931>

Pembleton LW, Cogan NOI, Forster JW (2013) StAMPP: an R package for calculation of genetic differentiation and structure of mixed-ploidy level populations. *Mol Ecol Resources* 13 (5):946–952. <https://doi.org/10.1111/1755-0998.12129>

Piedallu C, Dallery D, Bresson C, Legay M, Gégout JC, Pierrat R (2023) Spatial vulnerability assessment of silver fir and Norway spruce dieback driven by climate warming. *Landscape Ecology* 38 (2):341–361. <https://doi.org/10.1007/s10980-022-01570-1>

Popko J, Hänsch R, Mendel RR, Polle A, Teichmann T (2010) The role of abscisic acid and auxin in the response of poplar to abiotic stress. In *Plant Biology* 12 (2):242–258. <https://doi.org/10.1111/j.1438-8677.2009.00305.x>

Postolache D, Oddou-Muratorio S, Vajana E, Bagnoli F, Guichoux E, Hampe A et al. (2021): Genetic signatures of divergent selection in European beech (*Fagus sylvatica* L.) are associated with the variation in temperature and precipitation across its distribution range. *Mol Ecol* 30 (20):5029–5047. <https://doi.org/10.1111/mec.16115>

Pritchard JK, Stephens M, Donnelly P (2000) Inference of Population Structure Using Multilocus Genotype Data. *Genetics* 155(2): 945–959. <https://doi.org/10.1093/genetics/155.2.945>

Raj A, Stephens M, Pritchard JK (2014) fastSTRUCTURE: variational inference of population structure in large SNP data sets. *Genetics* 197 (2):573–589. <https://doi.org/10.1534/genetics.114.164350>

Rellstab C, Gugerli F, Eckert AJ, Hancock AM, Holderegger R (2015) A practical guide to environmental association analysis in landscape genomics. *Mol Ecol* 24 (17):4348–4370. <https://doi.org/10.1111/mec.13322>

R Core Team. R: A Language and Environment for Statistical (2024) <https://CRAN.R-project.org/>.

Rhee SY, Osborne E, Poindexter PD, Somerville CR (2003) Microspore separation in the quartet 3 mutants of *Arabidopsis* is impaired by a defect in a developmentally regulated polygalacturonase required for pollen mother cell wall degradation. *Plant Physiology* 133 (3):1170–1180. <https://doi.org/10.1104/pp.103.028266>.

Rukh S, Sanders TGM, Krüger I, Schad T, Bolte A (2023) Distinct Responses of European Beech (*Fagus sylvatica* L.) to Drought Intensity and Length—A Review of the Impacts of the 2003 and 2018–2019 Drought Events in Central Europe. *Forests* 14 (2). <https://doi.org/10.3390/f14020248>

Scaglione D, Pinosio S, Marroni F, Di Centa E, Fornasiero A, Magris G et al. (2019) Single primer enrichment technology as a tool for massive genotyping: a benchmark on black poplar and maize. *Annals of Botany* 124 (4):543–552. <https://doi.org/10.1093/aob/mcz054>

Sdano MA, Fulcher JM, Palani S, Chandrasekharan MB, Parnell TJ, Whitby FG. et al. (2017) A novel SH2 recognition mechanism recruits Spt6 to the doubly phosphorylated RNA polymerase II linker at sites of transcription. *In eLife* 6. <https://doi.org/10.7554/eLife.28723>

Seo M, Koiwai H, Akaba S et al. (2000) Abscisic aldehyde oxidase in leaves of *Arabidopsis thaliana*. *Plant J* 23:481–488. <https://doi.org/10.1046/j.1365-313x.2000.00812.x>

Sun BB, Kurki MI, Foley CN et al. (2022) Genetic associations of protein-coding variants in human disease. *Nature* 603:95–102. <https://doi.org/10.1038/s41586-022-04394-w>

Talajić A, Dominko K, Lončarić M, Ambriović-Ristov A, Četković H (2024) The ancestral type of the R-RAS protein has oncogenic potential. *In Cellular & Molecular Biology Letters* 29 (1). <https://doi.org/10.1186/s11658-024-00546-0>

Tost M, Grigoriadou-Zormpa O, Wilhelmi S, Beissinger T, Targem MB, Müller M, Wildhagen H, Curtu AL, Gailing O (2025) Genome-wide association study in European beech (*Fagus sylvatica* L.) for drought stress traits. PREPRINT (Version 2) available at bioRxiv [<https://www.biorxiv.org/content/10.1101/2025.04.08.647712v1>].

Tylewicz S, Petterle A, Marttila S, Miskolczi P, Azeez A, Singh RK et al. (2018) Photoperiodic control of seasonal growth is mediated by ABA acting on cell-cell communication. *In Science* 360 (6385):212–215. <https://doi.org/10.1126/science.aan8576>

van Dijk E, Hoogeveen A, Abeln S (2015) The hydrophobic temperature dependence of amino acids directly calculated from protein structures. *PLoS Comput Biol* 11 (5). <https://doi.org/10.1371/journal.pcbi.1004277>

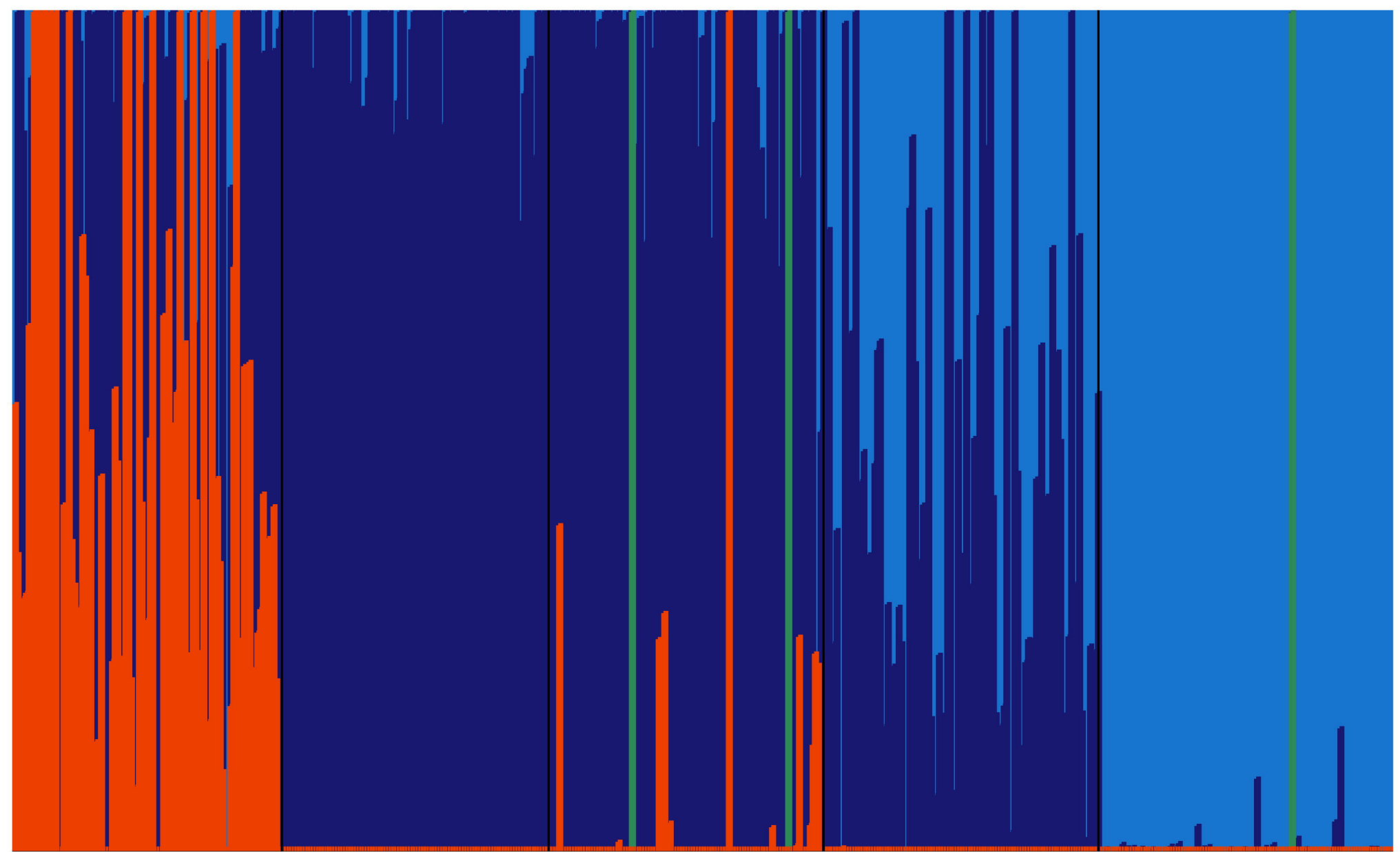
Van Rossum G, Drake PL (2009) Python 3 Reference Manual, Scotts Valley, CA: CreateSpace.

Watanabe S, Takahashi N, Kanno Y, Suzuki H, Aoi Y, Takeda-Kamiya N et al. (2020) The *Arabidopsis* NRT1/PTR FAMILY protein NPF7.3/NRT1.5 is an indole-3-butyric acid transporter involved in root gravitropism. *Proc Natl Acad Sci USA* 117 (49):31500–31509. <https://doi.org/10.1073/pnas.2013305117>.

Xu YW, Bhargava G, Wu H, Loeber G, Tong L (1999) Crystal structure of human mitochondrial NAD(P)⁺-dependent malic enzyme: a new class of oxidative decarboxylases. *Structure* 7 (8):877–889. [https://doi.org/10.1016/S0969-2126\(99\)80115-4](https://doi.org/10.1016/S0969-2126(99)80115-4)

Yang J, Manolio T, Pasquale LR, Boerwinkle E, Caporaso N, Cunningham JM et al. (2011) Genome partitioning of genetic variation for complex traits using common SNPs. *Nature Genetics* 43 (6):519–525. <https://doi.org/10.1038/ng.823>

Yu DC, Chen XY, Li X, Zhou HY, Yu DQ, Yu XL et al. (2021) Transcript levels of spindle and kinetochore-associated complex 1/3 as prognostic biomarkers correlated with immune infiltrates in hepatocellular carcinoma. *Scientific Reports* 11 (11165). <https://doi.org/10.1038/s41598-021-89628-z>



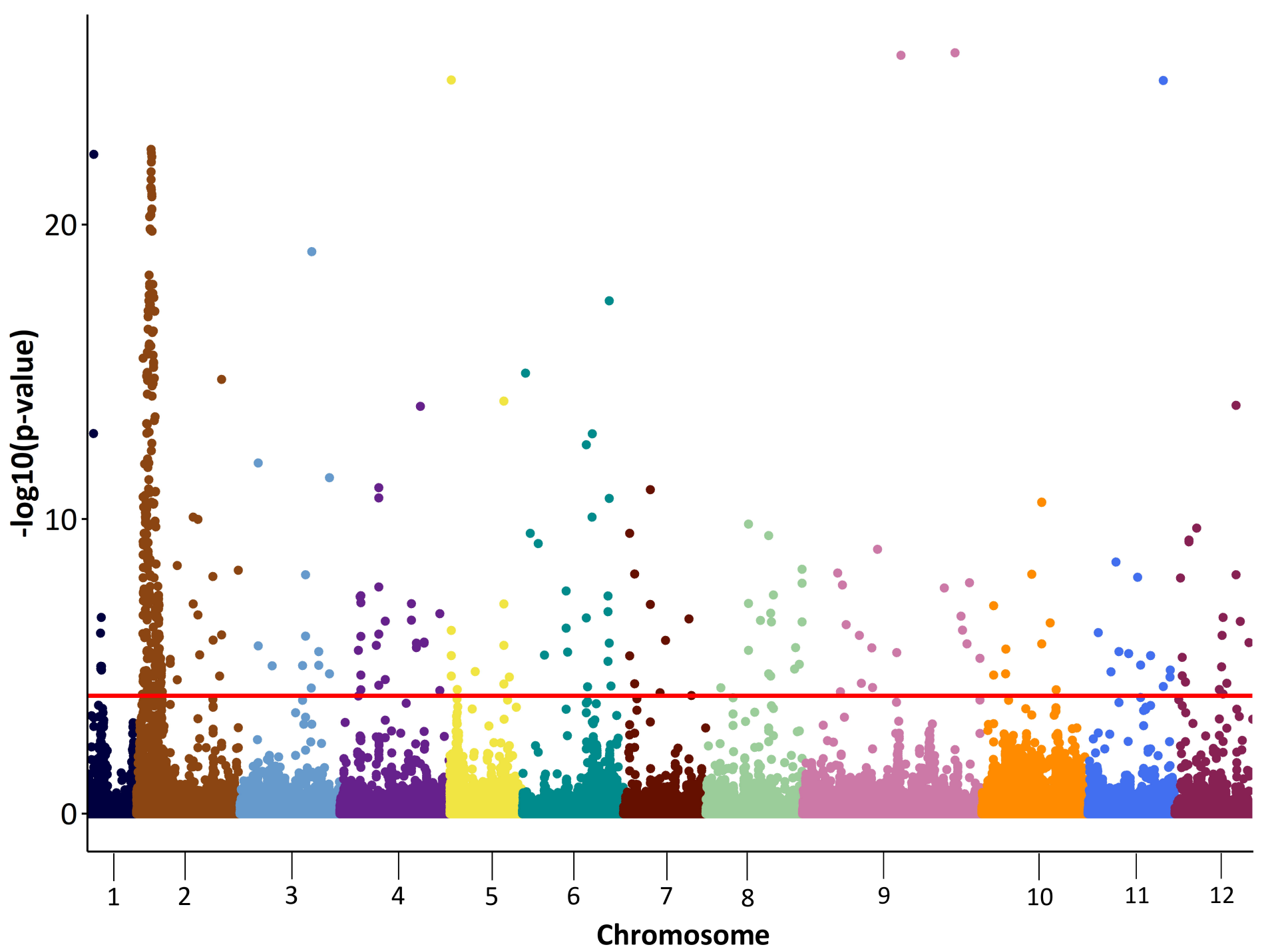
Lempes

Tampa

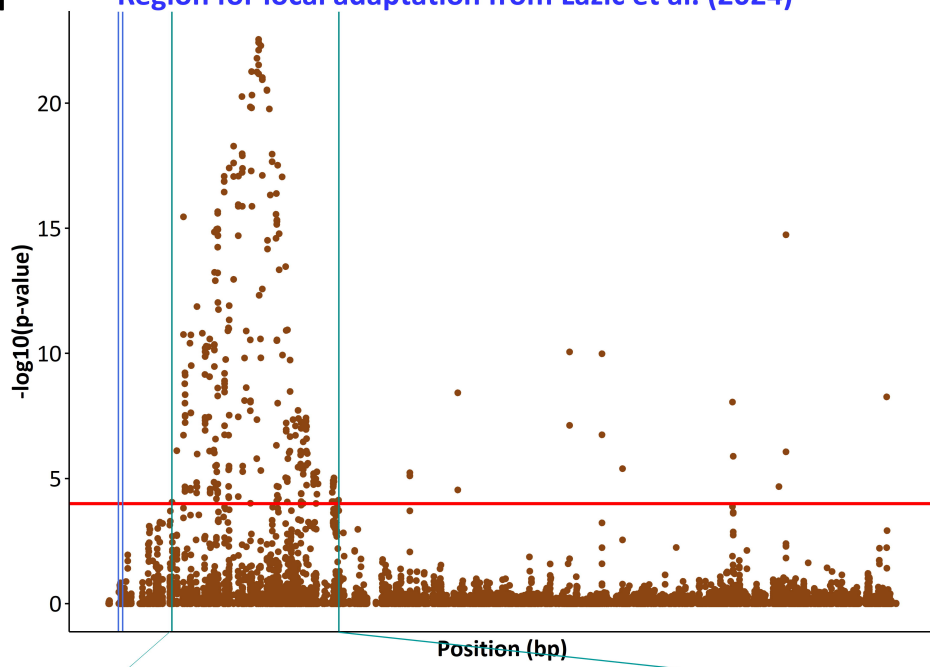
Solomon

Lupului

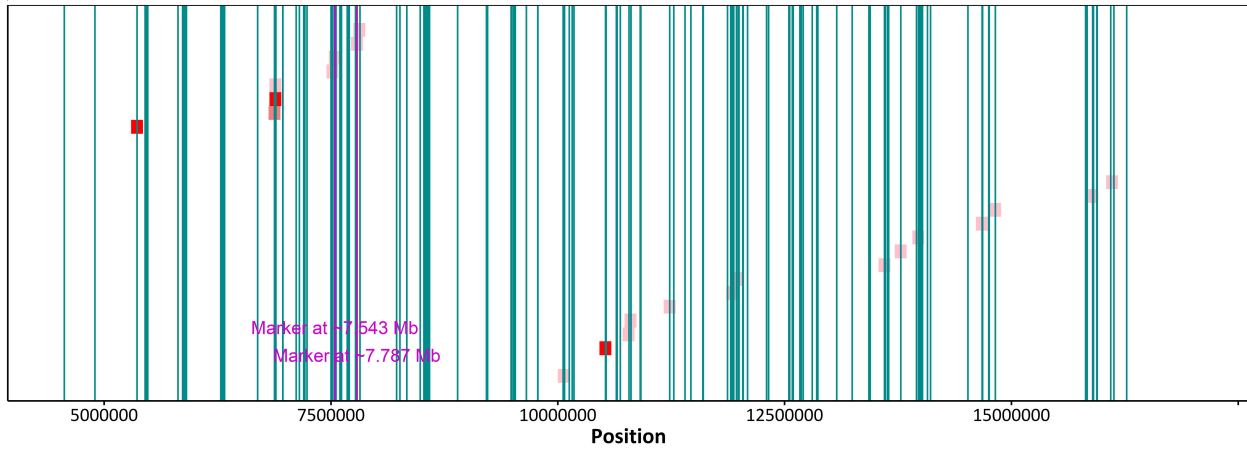
Ruia



a Region for local adaptation from Lazic et al. (2024)



b



c

